SPHERICAL NEAR-FIELD MEASUREMENTS AT UHF FREQUENCIES WITH COMPLETE UNCERTAINTY ANALYSIS

Allen Newell, Patrick Pelland
Nearfield Systems Inc.
19730 Magellan Drive,
Torrance, CA 90502-1104

Brian Park, Ted White, Amanual Haile
The Boeing Company
2060 E Imperial Highway
El Segundo, CA 90245

ABSTRACT

A spherical near-field measurement range at Nearfield Systems Inc. has recently been used to measure gain, pattern and polarization of a multi-element helix array operating in the UHF band. Verification of gain performance over the operating band was of primary importance and so major efforts were made to obtain the best possible gain results and to quantify the gain uncertainty through a complete error analysis. A single element helix gain standard was first calibrated and the estimated uncertainty in this calibration was 0.35 dB. A double ridged horn was to be used as the probe for the spherical near-field measurements and so the patterns of the horn at all test frequencies were measured on the spherical range using identical horns as the AUT and the probe. From these measurements, probe pattern files were generated that could be used to perform the probe correction in the measurements of the helix gain standard and the multi-element array. The helix gain standard was then installed in a new spherical near-field range at NSI with the double ridged horn as the probe. The range used a specially designed phi-over theta rotator that could support and rotate the array and maintain the required position accuracy. The chamber was lined with 36 inch absorber. Spherical measurements were then performed and the data processed to provide the far-field peak amplitudes at each frequency that were necessary for gain measurements. The far-field peak values are equivalent to the far electric field for the gain standard and are compared to the same parameter for the multi-element array to produce the final gain results. The helix array was then installed in the spherical range and a series of measurements were performed to produce the far-field gain, pattern and polarization results and also to provide the data for the complete 18 term uncertainty analysis. The uncertainty in the gain measurements was 0.45 dB and the axial ratio uncertainty was 0.11 dB.

Keywords: near-field, measurements, spherical, UHF band, gain, uncertainty analysis.

1.0 Introduction

Accurate and reliable gain measurements over the full operating bandwidth of a communication antenna are one of the most important parameters required in its qualification and testing. Gain is also one of the most difficult parameters to measure accurately and this is especially true for operating frequencies in the UHF band. Interference and scattering are difficult to control on an outdoor range, and for large aperture antennas, it is difficult to produce a uniform field in an anechoic chamber or a compact range. In the measurements reported here, a spherical near-field range[1] was used where the sources of error could be controlled and thoroughly evaluated in order to produce a high confidence in the gain, pattern and polarization results.

2.0 Near-field Test Range

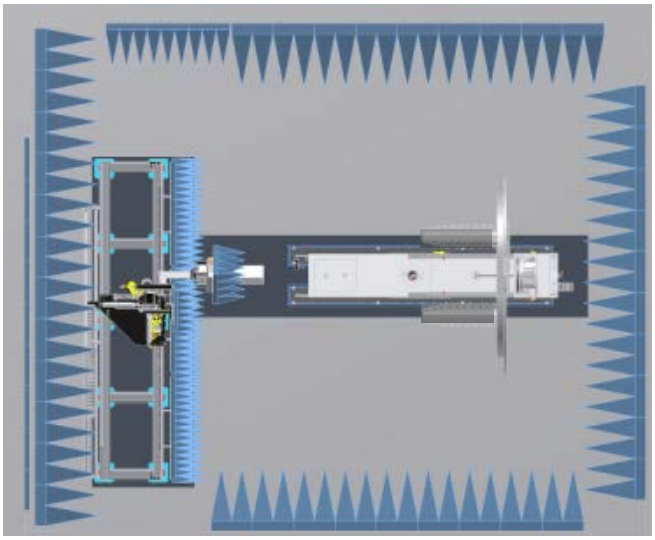

Figure 1 Spherical near-field chamber.

The spherical test range is a new facility recently installed at Nearfield Systems Inc. (NSI) to accommodate the current and future measurement requirements for large antennas and frequency ranges from 200 MHz to 50 GHz using spherical near-field measurement. The chamber shown in Figure 1 and is 29.5 ft long, 24.5 ft wide and 21 ft high and is covered with 36 inch pyramidal absorber. The phi over theta rotator is designed to handle loads up to 650 lbs with a position accuracy of at least 0.03 degrees.

3.0 Helix Array Test Antenna, Helix Gain Standard and Horn Near-Field Probe

The Antenna Under Test (AUT) is a four element helix array shown in Figures 2 and 3.

Figure 2 Four element helix array test antenna.

Figure 3 Four element helix array test antenna.

The gain standard was a single element helix antenna shown in Figure 4 as it was mounted in the spherical near-field range.

Figure 4 Single element helix gain standard in the spherical near-field chamber with the horn probe.

The probe for the spherical near-field measurements was a dual ridged horn shown in Figures 4 and 5. In Figure 5, a nominally identical horn is being used as a probe for the pattern measurements that were needed to produce the probe correction files. The horn on the left is in the AUT position for pattern measurements and the aperture of the horn is covered with absorber to reduce the effect of multiple reflections. The details of the use of the absorber over the aperture will be discussed later.

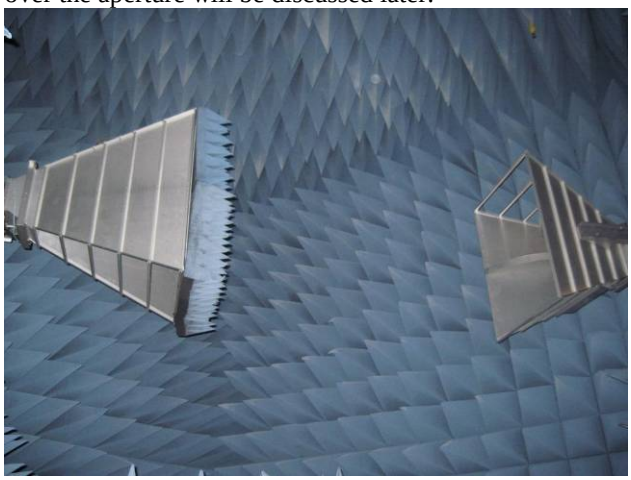

Figure 5 Two dual ridged horns in the spherical chamber during the probe pattern measurements.

4.0 . Measurement Sequence

Gain Standard Calibration The first measurements were performed on the helix gain standard on another range before the antennas were installed in the near-field chambers. A three antenna gain measurement[2] was used to determine the gain of the standard where one of the other antennas was a nominally identical single element

helix and the third antenna was a single element helix with a different design. The gain could be determined from both the three antenna measurements and from a two antenna method assuming identical antennas. The results of these measurements produced gain values with an estimated uncertainty of 0.35 dB.

Probe Pattern Measurements The two horns were then installed in the near-field anechoic chamber as shown in Figure 5 and spherical near-field data obtained at each of the required measurement frequencies. The bandwidth of the measurements on the gain standard and the horn probes was extended to accommodate possible future use. The horn probe was characterized in two configurations that would make it possible to evaluate the effect of multiple reflections in the measurements on the gain standard and the helix array.

Because the measurement radii for the probe pattern, the gain standard and the final helix array measurements are on the order of three wavelengths, multiple reflections could be a significant source of error. The multiple reflections can in principle be evaluated by making a series of near-field measurements where the radius is changed in $\lambda/8$ steps. This was not practical in this case because of the long wavelength and the sizes of the three antennas. Past measurements have shown that when a horn is used as the probe, the effect of multiple reflections can be reduced by placing an absorber panel over the aperture of the horn as shown in Figure 5. Most of the reflections from the horn arise from the region inside the horn and especially the throat of the horn. An absorber panel with an attenuation of about 6-10 dB will significantly reduce the multiple reflections, and in this case the attenuation of the panel was on the order of 10 dB. The absorber panel does change the probe pattern slightly as shown in Figure 6 and so pattern measurements were taken with and without the absorber in place and probe correction files were produced for both configurations. The horn measurements without the absorber were taken first, the absorber panel was then installed and the pattern measurements repeated just prior to beginning the helix tests. This sequence ensured that the absorber was in the same configuration for both the pattern and helix measurements. Far-field patterns were computed from the data with and without the absorber panel in place and used to produce the probe pattern files that would be used for processing the spherical near-field data on the gain standard helix and the helix array.

Helix Gain Standard Measurements The horn without the absorber panel was then placed in the probe position

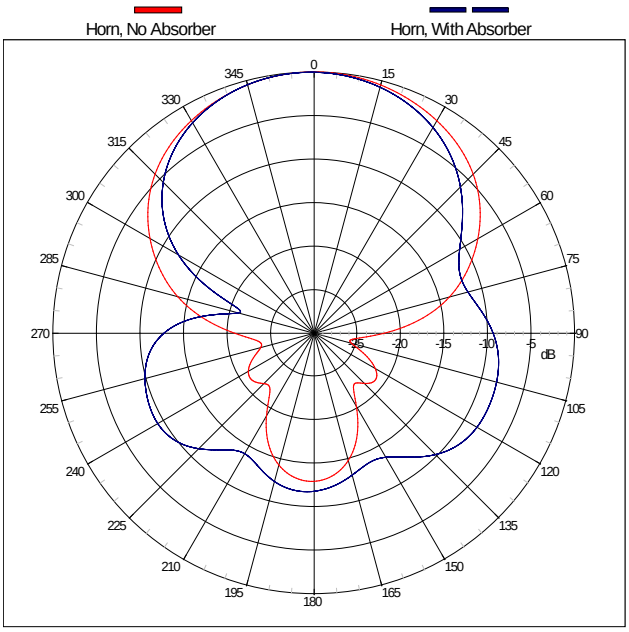

Figure 6 Horn probe far-field patterns with and without the absorber panel at 230 MHz.

and the helix gain standard was installed in the AUT position on the spherical near-field range as shown in Figure 4. Spherical near-field measurements were performed at all frequencies and the horn with the absorber was then installed and the measurements repeated. Comparison of the results from using the different probe facilitated analysis of multiple reflection effects.

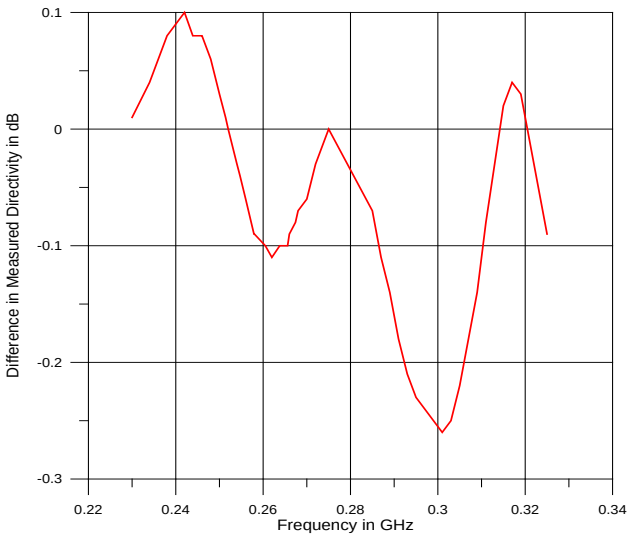

Figure 7 Directivity difference of gain standard from measurements with and without probe absorber.

Figure 7 shows the difference in the directivity of the gain standard from measurements with the two probe

configurations. The period of the difference curve ripple indicates a 4 m spacing between the reflection sources associated with the gain standard and the horn. This is consistent with the 3.8 m measurement radius and the length of the horn. The 0.1 dB amplitude of the ripple is used as an estimate of the multiple reflection error in both the directivity and the gain standard far-field peak that is used for comparison gain calculations.

The radius of the minimum sphere for the helix gain standard indicated a required angular spacing of 30 degrees, but oversampling with a spacing of 7.5 degrees was used to allow processing using all the data and subsets with larger spacing to estimate the uncertainty due to data point spacing. Redundant sampling over the full sphere was used where the spans in both theta and phi were 360 degrees and this produced two measurements at each point on the sphere. The redundant data could then be averaged to reduce and evaluate errors due to chamber scattering.

Helix Array Measurements The helix array was then installed on the spherical near-field range and redundant, oversampled near-field data obtained using both horn probe configurations. Patterns, directivity, far-field peak and axial ratio were then calculated for each data set. The gain was a critical parameter and so it was calculated using three different methods. The first method used the directivity results from the near-field measurements and the ohmic loss of the array from measurements on the feed networks and the helix elements. The second method was a gain comparison techniques using the far-field peak values of the gain standard and the helix array along with the gain of the standard. The third method used a direct gain technique where the horn probe was the gain standard and the range insertion loss was measured by connecting the AUT input cable and the probe output cable. The gain of the horn probe was determined from the probe pattern near-field measurements using one horn as the AUT and the other as the probe. The insertion loss was also determined for these measurements and the gain of the horns calculated from the direct gain equation assuming identical AUT and probe.

5.0 Measurement Results

Figure 8 shows the gain results for the three different methods along with the predicted gain based on the theoretical model. All of the results agree within the estimated uncertainty that will be discussed in more detail in a later section. Figure 9 compares the predicted axial ratio with the results from the measurements. The sample far-field patterns in Figure 10 shows excellent agreement with the predicted patterns for both main and cross polarization. The absence of any high frequency ripple on the patterns that often appears on measurements in this frequency band indicates the high quality of the results.

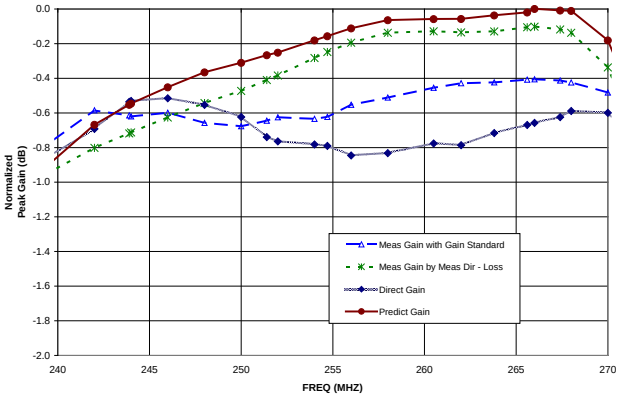

Figure 8 Gain variation results for three measurement methods compared to predicted gain.

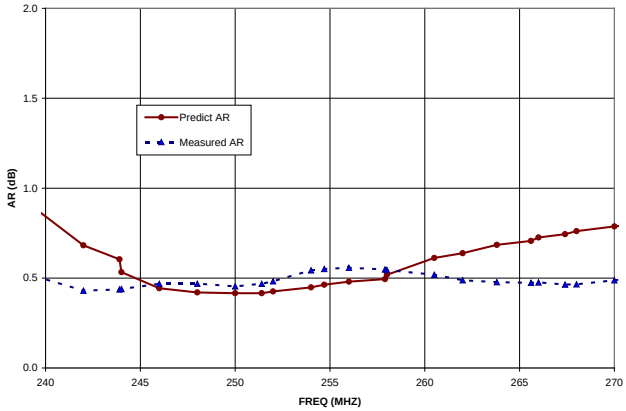

Figure 9 Axial ratio results compared to predicted values.

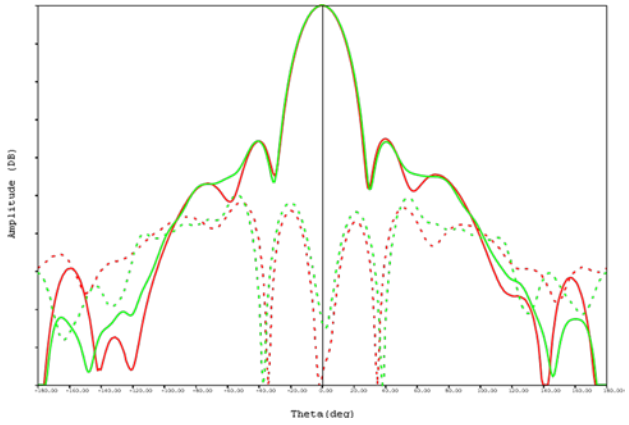

Figure 10 Pattern results compared to predicted patterns.

6.0 Uncertainty Analysis

The NIST 18 term uncertainty model[3] applied to spherical measurements was used as the basis for estimating

uncertainties in the far-field results. Equation (1) for determining gain using the comparison technique identifies the four terms that will contribute to the uncertainty in the final gain results using this method. As previously noted the estimated uncertainty in the gain of the standard is 0.35 dB. The primary error sources for the far-field peaks of the gain standard and the array are multiple reflections between the probe and the AUT, room scattering from the absorber walls, position errors, data point spacing, receiver non-linearity, probe pattern, leakage signals from transmission components and random errors.

$$G_A = FFP_A - FFP_S + G_s + M$$

where

G_A = AUT Gain, G_S = Gain of Standard

FFP_A = Far Field Peak for AUT

FFP_S = Far Field Peak for Standard

M=Mismatch correction (1.1)

The use of the data with and without the absorber over the probe aperture to estimate the effect of multiple reflections has already been discussed. Room scattering effects in the measured near-field data are analyzed by comparing near-field cuts for ϕ=0 and ϕ=180 degrees as illustrated in Figure 11.

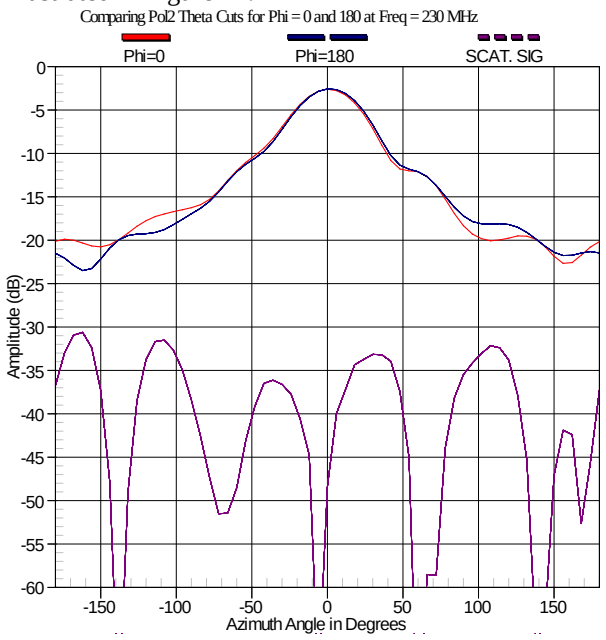

Figure 11 Estimating room scattering for near-field data on helix gain standard.

The room scattering effect on the far-field parameters is reduced by using the oversampled redundant data and is estimated by comparing far-field patterns and directivity using the full redundant data and a non-redundant subset of the data. The effect of position errors is estimated by comparing far-field results using unmodified near-field data with modified data that has an imposed position errors. The data point spacing effect was estimated by using the full measured data and a subset using every other data point. The receiver non-linearity was estimated using a series of measurements at different power levels and a derived non-linearity was applied to a data set. The far-field results with and without the simulated non-linearity quantified its effect on these results. The probe pattern uncertainty effect was estimated by computing and comparing the far-fields using two different probe pattern files for the probe correction. One file was for the correct measurement frequency and the other was for a frequency where the pattern change was larger than the estimated uncertainty in the probe pattern measurements. Near-field leakage data was obtained with either the AUT input or the probe output transmission lines terminated. This data was processed by the spherical software to produce the far-field patterns due to leakage signals and its level compared to the AUT far-field levels. Random errors were estimated from a series of repeat measurements. Table 1 summarizes the results of the uncertainty analysis on the gain standard measurements and Table 2 lists the terms for the comparison gain measurement on the helix array.

Table 1 Estimated uncertainties in the far-field peak of the gain standard.

Error Source	Estimated Uncertainty dB
Multiple Reflections	0.10
Room Scattering	0.15
Position Errors	0.05
Data Point Spacing	0.02
Receiver Non-Linearity	0.05
Probe Pattern	0.06
Leakage	0.02
Random	0.02
RSS Combination	**0.20**

Table 2 Estimated uncertainties in the helix array gain using the comparison gain technique.

Error Source	Estimated Uncertainty dB
Gain of the Gain Standard	0.35
Gain Standard FF Peak	0.20
Impedance Mismatch	0.10
Multiple Reflections	0.10
Room Scattering	0.10
Position Errors	0.05
Data Point Spacing	0.05
Receiver Non-Linearity	0.02
Probe Pattern	0.07
Leakage	0.02
Random	0.02
RSS Combination	**0.45**

7.0 **Summary**

Measurements on a large helix array operating in the UHF frequency range have been successfully completed using spherical near-field techniques. A careful and complete uncertainty analysis has been performed that estimates an uncertainty of 0.45 dB in the gain results. The results show excellent agreement with predicted values.

8.0 **References**

[1] Hansen, J.E., ed. *Spherical Near Field Antenna Measurements*, Peregrinus, London, 1988**.**

[2] Newell, A.C.; Ward, R.D.; McFarlane, E.J., "Gain and Power Parameter Measurements Using Planar Near-Field Techniques," *IEEE Transactions on Antennas and Propagation, Vol.* AP-36, No. 6, pp. 792-803, June 1988.

[3] Newell, A.C., "Error analysis techniques for planar near-field measurements," *IEEE Transactions on* Antennas and *Propagation, Vol.* AP-36, pp. 755-768, June 1988.